AD-A162 834 APPLICATIONS OF DIFFERENTIAL TOPOLOGY TO GRID GENERATION(U) FLORIDA UNIV GAINESVILLE D C WILSON 25 NOV 85 AFOSR-TR-85-1165 AFOSR-83-0158 1/1

UNCLASSIFIED F/G 12/1 NL

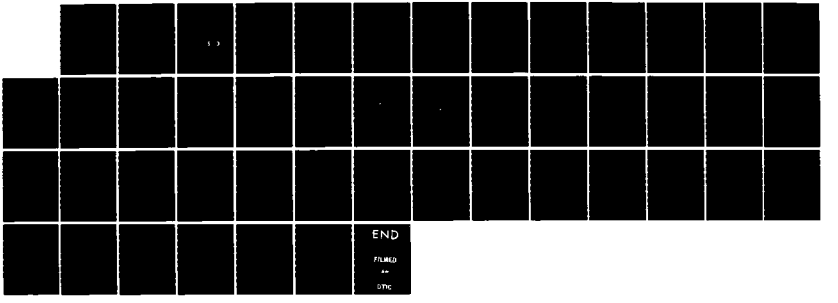

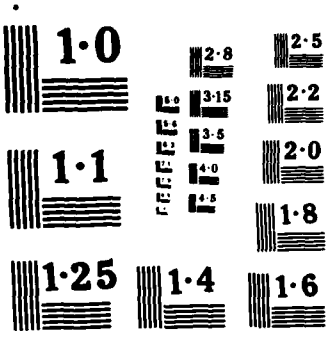

NATIONAL BUREAU OF STANDARDS
MICROCOPY RESOLUTION TEST CHART

UNCLASSIFIED

SECURITY CLASSIFICATION

AD-A162 834

ION PAGE

1a. REPORT SECURITY CLAS
UNCLASSIFIED

TRICTIVE MARKINGS

2a. SECURITY CLASSIFICATION AUTHORITY

3. DISTRIBUTION/AVAILABILITY OF REPORT
Approved for public release; distribution unlimited.

2b. DECLASSIFICATION/DOWNGRADING SCHEDULE

4. PERFORMING ORGANIZATION REPORT NUMBER(S)

5. MONITORING ORGANIZATION REPORT NUMBER(S)
AFOSR-TR- 85-1165

6a. NAME OF PERFORMING ORGANIZATION
University of Florida

6b. OFFICE SYMBOL (If applicable)

7a. NAME OF MONITORING ORGANIZATION
Air Force Office of Scientific Research

6c. ADDRESS (City, State and ZIP Code)
Gainesville, FL 32611

7b. ADDRESS (City, State and ZIP Code)
Directorate of Mathematical & Information Sciences, Bolling AFB DC 20332-6448

8a. NAME OF FUNDING/SPONSORING ORGANIZATION
AFOSR

8b. OFFICE SYMBOL (If applicable)
NM

9. PROCUREMENT INSTRUMENT IDENTIFICATION NUMBER
AFOSR-83-0158

8c. ADDRESS (City, State and ZIP Code)
Bolling AFB DC 20332-6448

10. SOURCE OF FUNDING NOS.

PROGRAM ELEMENT NO.	PROJECT NO.	TASK NO.	WORK UNIT NO.
61102F	2304	D9	

11. TITLE (Include Security Classification)
Applications of Differential Topology to Grid Generation

12. PERSONAL AUTHOR(S)
Professor Wilson

13a. TYPE OF REPORT	13b. TIME COVERED	14. DATE OF REPORT (Yr., Mo., Day)	15. PAGE COUNT
Final	FROM 1 Jun 83 TO 31May84	November 25, 1985	47

16. SUPPLEMENTARY NOTATION

17. COSATI CODES			18. SUBJECT TERMS (Continue on reverse if necessary and identify by block number)
FIELD	GROUP	SUB. GR.	giid generation, smoothing techniques

19. ABSTRACT (Continue on reverse if necessary and identify by block number)

This minigrant involved a study of how smoothing techniques can be utilized in the area of grid generation. It was shown how one global grid can be patched together from a number of smaller ones. The paper "Applications of differential topology to grid generation" constituted the final report for this effort. This paper was revised and renamed "Smoothing patched grids".

20. DISTRIBUTION/AVAILABILITY OF ABSTRACT
UNCLASSIFIED/UNLIMITED ☒ SAME AS RPT. ☐ DTIC USERS ☐

21. ABSTRACT SECURITY CLASSIFICATION
UNCLASSIFIED

22a. NAME OF RESPONSIBLE INDIVIDUAL	22b. TELEPHONE NUMBER (Include Area Code)	22c. OFFICE SYMBOL
Captain John P. Thomas Jr.	(202) 767-5026	NM

DD FORM 1473, 83 APR EDITION OF 1 JAN 73 IS OBSOLETE.

UNCLASSIFIED

SECURITY CLASSIFICATION OF THIS PAGE

AFOSR-TR- 85-1165

FINAL REPORT

(2)

Applications of Differential Topology to Grid Generation

D.C. Wilson
University of Florida

Abstract

The purpose of this paper is to indicate how smoothing techniques from Differential Topology can be applied to the area of grid generation in Computational Fluid Dynamics. The basic method is to patch together one global grid from a number of smaller ones. The smoothing theory allows one to blend the grid from one section into the grid of an adjacent one.

This Research was supported in part by AFOSR Grant #83-0158.

I. Introduction

The author developed the ideas outlined in this paper while attempting to construct an algebraic grid[1] for the X-24C aircraft. (See Figure 1.) In a natural way this plane can be divided into the forebody, the body, and the airfoil. The forebody can be further divided into the nose and the canopy. The airfoil region can be subdivided into the airfoil and the body adjacent to it. The frustration of trying to blend these various pieces together into one large grid drove the author to search for a technique of approximating one-to-one continuous functions (i.e. homeomorphisms) by one-to-one smooth functions (i.e. diffeomorphisms). Techniques lifted from the Differential Topology books by Hirsch[2] and Munkres[3] provide the foundation for the theorems and ideas presented in Section II. Theorems 2.1 and 2.3 guarantee that any continuous transformation can be approximated arbitrarily closely by a smooth one. Theorems 2.4 and 3.1 can be used to ensure that the approximation will have non-zero Jacobian. Theorem 2.5 ensures that the approximation of an orthogonal grid will be almost orthogonal.

To apply the smoothing theory to grid generation a large number of double (or triple) integrals must be computed. Theorem 3.2 is the 2-dimensional version of Simpson's Rule which was used to calculate the convolutions at the various grid points for the examples pictured at the end of the paper. While other more sophisticated methods (e.g. iterated Romberg) could be

used, the author chose Simpson because of its simplicity and rapid rate of convergence.

II. The Smoothing Theory

An excellent reference for the Advanced Calculus needed in this section is Rudin[4]. While the theorems are all stated for two dimensions, they are all valid in n dimensions.

The smoothing techniques from Differential Topology involve a convolution with a "bump" function. While there are innumerable choices for a bump function (e.g. cubic B-splines), the one indicated below proved convenient.

Definition. $$\alpha(x) = \begin{cases} 0 & \text{if } x \leq 0 \\ e^{-1/x} & \text{if } x > 0 \end{cases}$$

The real valued function α is C^∞ (i.e. All higher derivatives exists); the graph of α is indicated in Figure 2.

If $a < b$, then define $\beta(x) = \alpha(x - a) \cdot \alpha(b - x)$. The function β is also C^∞; its graph is indicated in Figure 3. Since we want the interval $[a,b]$ to be symmetric about zero, we define $$\beta_p(x) = \begin{cases} \text{EXP}(-p^2/(p^2 - x^2)) & \text{if } |x| < p \\ 0 & \text{if } |x| \geq p, \end{cases}$$ where the parameter $p > 0$. If $A_p = \int_{-p}^{p} \beta_p(x)dx$ and $\theta_p(x) = \beta_p(x)/A_p$, then $\theta_p(x)$ is a C^∞ bump function such that $\int_{-p}^{p} \theta_p(x)dx = 1$. The function $\theta_p(x,y) = \theta_p(x) \cdot \theta_p(y)$ is a bump function of two variables such that $\int_{-p}^{p}\int_{-p}^{p} \theta_p(x,y)dxdy = 1$.

Let R_p denote the square $[-p,p] \times [-p,p]$.

Definition. If $F(\xi,\eta)$ is a piecewise continuous function from $R^2 \to R$, the convolution of F by θ_p is:

$$\theta_p * F(\xi,\eta) = \iint_{R_p} F(\xi-u,\ \eta-v)\cdot\theta_p(u,v)\,du\,dv.$$

This convolution can be thought of as an "average" of the values F near (ξ,η). Heuristically, Theorem 2.1 states that if p is "small", then $\theta_p * F$ is "close" to F.

Theorem 2.1.

If F is continuous, $\varepsilon > 0$, and $|F(\xi-u,\ \eta-v) - F(\xi,\eta)| \le \varepsilon$ for all $(u,v) \in R_p$, then $|\theta_p * F(\xi,\eta) - F(\xi,\eta)| \le \varepsilon$.

Proof.

The result follows from the following sequence of equalities and inequalities.

$$|\theta_p * F(\xi,\eta) - F(\xi,\eta)|$$

$$= \left|\iint_{R_p} F(\xi-u,\ \eta-v)\theta_p(u,v)\,du\,dv - F(\xi,\eta)\right|$$

$$\le \iint_{R_p} \theta_p(u,v)\cdot|F(\xi-u,\ \eta-v) - F(\xi,\eta)|\,du\,dv$$

$$\le \varepsilon\iint_{R_p} \theta_p(u,v)\,du\,dv = \varepsilon.$$

Theorem 2.2 shows that if p is "small" and $\frac{\partial F(\xi,\eta)}{\partial \xi}$ is is continuous at (ξ,η) then $\frac{(\theta_p * F(\xi,\eta))}{\partial \xi}$ is "close" to $\frac{\partial F(\xi,\eta)}{\partial \xi}$. Note that Theorem 2.2 can be easily generalized to higher derivatives.

Theorem 2.2.

If $F(\xi,\eta)$ is C^1, then $\frac{(\theta_p * F(\xi,\eta))}{\partial \xi} = \theta_p * \frac{\partial F(\xi,\eta))}{\partial \xi}$.

Moreover, if $\epsilon > 0$ and $\left|\frac{\partial F(\xi-u,\ \eta-v)}{\partial \xi} - \frac{F(\xi,\eta)}{\partial \xi}\right| \leq \epsilon$ for $(u,v) \in R_p$, then $\left|\frac{\partial \Theta_p * F(\xi,\eta)}{\partial \xi} - \frac{\partial F(\xi,\eta)}{\partial \xi}\right| \leq \epsilon$.

Proof.

Since $\frac{\partial}{\partial \xi} \iint_{R_p} \Theta_p(u,v)F(\xi-u,\ \eta-v)dudv = \iint_{R_p} \Theta_p(u,v)\cdot\frac{\partial F(\xi-u,\eta-v)}{\partial \xi}\ dudv$, $\frac{\partial \Theta_p * F(\xi,\eta)}{\partial \xi} = \Theta_p * \frac{F(\xi,\eta)}{\partial \xi}$. The second half of the theorem follows from the proof of Theorem 2.1.

Remark.

Theorem 2.2 could have been phrased as follows: If $\frac{\partial F}{\partial \xi}$ is piecewise continuous and $m \leq \frac{\partial F}{\partial \xi} \leq M$, then $m \leq \Theta_p * \frac{\partial F}{\partial \xi} \leq M$. Thus, at points where $\frac{\partial F}{\partial \xi}$ is not continuous, the convolution of F by Θ_p "blends" the first partials of the grid in one section into those of the next. This blending also occurs for all higher derivatives.

Theorem 2.3.

If $F(\xi,\eta)$ is piecewise continuous, then $\Theta_p * F(\xi,\eta)$ is C^∞.

Proof.

By change of variables we have

$$\frac{\partial \Theta_p * F(\xi,\eta)}{\partial \xi} = \frac{\partial}{\partial \xi} \iint_{R_p} \Theta_p(u,v)\cdot F(\xi-u,\ \eta-v)dudv$$

$$= \frac{\partial}{\partial \xi} \int_{\eta-p}^{\eta+p} \int_{\xi-p}^{\xi+p} \Theta_p(\xi+u,\ \eta+v)\ F(u,v)dudv$$

$$= \int_{\eta-p}^{\eta+p} \int_{\xi-p}^{\xi+p} \frac{\partial\ \Theta_p(\xi+u,\ \eta+v)}{\partial \xi} \cdot F(u,v)dudv.$$

Since Θ_p is C^∞, $\Theta_p * F$ is C^∞.

Theorem 2.4 ensures that if T is one-to-one and p is "small", then $\Theta_p * T$ is one-to-one.

Theorem 2.4.

If $T(\xi,\eta) = (X(\xi,\eta), Y(\xi,\eta))$ where $X(\xi,\eta)$ and $Y(\xi,\eta)$ are C^1, then if the Jacobian J of T is not zero there is a $p > 0$ such that the Jacobian J_p of $\Theta_p * T(\xi,\eta) = (\Theta_p * X(\xi,\eta), \Theta_p * Y(\xi,\eta))$ is not zero.

Proof.

The Jacobain $J_p = (\Theta_p * \frac{\partial X}{\partial \xi}) \cdot (\Theta_p * \frac{\partial Y}{\partial \eta}) - (\Theta_p * \frac{\partial X}{\partial \eta}) \cdot (\Theta_p * \frac{\partial Y}{\partial \xi})$.

By Theorem 2.2 $\lim_{p \to 0} J_p = J$.

Theorem 2.5.

Let $T(\xi,\eta) = (X(\xi,\eta) , Y(\xi,\eta))$ be a C^1 transformation and let Ψ be the angle between $u = (\frac{\partial X}{\partial \xi}, \frac{\partial Y}{\partial \xi})$ and $v = (\frac{\partial X}{\partial \eta} , \frac{\partial Y}{\partial \eta})$.

If Ψ_p denotes the angle between $u_p = (\Theta_p * \frac{\partial X}{\partial \xi} , \Theta_p * \frac{\partial Y}{\partial \xi})$ and

$v_p = (\Theta_p * \frac{\partial X}{\partial \eta} , \Theta_p * \frac{\partial Y}{\partial \eta})$, then $\lim_{p \to 0} \Psi_p = \Psi$.

Proof.

By Theorem 2.2 $\lim_{p \to 0} u_p = u$ and $\lim_{p \to 0} v_p = v$. Since $\cos \Psi_p = \frac{u_p \cdot v_p}{|u_p| \cdot |v_p|}$

and $\cos \Psi = \frac{(u \cdot v)}{|u| \cdot |v|}$, $\lim_{p \to 0} \Psi_p = \Psi$.

Theorem 2.6.

If $F(\xi,\eta) = F_1(\xi,\eta) + F_2(\xi,\eta)$, where F_1 and F_2 are piecewise continuous, then $\Theta_p * F(\xi,\eta) = \Theta_p * F_1(\xi,\eta) + \Theta_p * F_2(\xi,\eta)$.

Proof.

The additivity of the integral is all that is needed to prove this theorem.

Theorem 2.7.

If $F(\xi,\eta) = f(\xi) \cdot g(\eta)$ where f and g are piecewise continuous, then $\Theta_p * F(\xi,\eta) = (\Theta_p * f(\xi)) \cdot (\Theta_p * g(\eta))$.

Proof.

This result is an immediate consequence of Fubini's Theorem.

Theorem 2.8.

If $F(\xi,\eta) = A + B\xi + C\eta + D\xi\eta$, then $\Theta_p * F(\xi,\eta) = F(\xi,\eta)$.

Proof.

It is a routine check to show that if $G(\xi,\eta) = \xi$, then $\Theta_p * G(\xi,\eta) = G(\xi,\eta)$. The theorem is now an immediate consequence of Theorems 2.6 and 2.7.

Theorem 2.8 shows that if a portion of the grid of the aircraft can de defined by equations of the form $F(\xi,\eta) = A + B\xi, + C\eta + D\xi\eta$ hen the convolution step can be bypassed. Thus, the grid can be generated much more rapidly in that region.

III. The Examples

Theorem 3.1.

If $T(\xi,\eta) = (X(\xi,\eta), Y(\xi,\eta))$ has piecewise continuous partials which satisfy $m_{11} \le \frac{\partial X}{\partial \xi} \le M_{11}$, $m_{12} \le \frac{\partial X}{\partial \eta} \le M_{12}$, $m_{21} \le \frac{\partial Y}{\partial \xi} \le M_{21}$, and $m_{22} \le \frac{\partial Y}{\partial \eta} \le M_{22}$ for points in $[u-p, u+p] \times [v-p, v+p]$, then

the Jacobian J_p of $\Theta_p * T$ is non-zero if either $m_{11}m_{22} - M_{21}M_{12} > 0$ or $M_{11}M_{22} - m_{12}m_{21} < 0$.

Proof.

By the remark after Theorem 2.2 $m_{11} \leq \Theta_p * \frac{\partial X(\xi,\eta)}{\partial \xi} \leq M_{11}$, etc. Since $m_{11}m_{22} - M_{12}M_{21} \leq J_p \leq M_{11}M_{22} - m_{12}m_{21}$, J_p is not zero.

Let $-p = x_0 < x_1 < \ldots < x_{2n} = p$ be a partition of $[-p,p]$ such that $x_{i+1} - x_i = h$ for all i. Let $y_j = x_j$. Let $A_{ij} = \{(i,j) | i,j \neq 0$ or $2n$ and either i or j odd$\}$. Let $B_{ij} = \{(i,j) |$ i or $j = 0$ or $2n\}$.

Theorem 3.2. (Simpson's Rule in 2-Dimensions)

If $F(u,v)$ is a C^4 function on R_p, then

$$\iint_{R_p} F(u,v)dudv = \tfrac{4}{3}h^2 \cdot \sum_{A_{ij}} F(x_i, y_j) + \tfrac{2}{3}h^2 \cdot \sum_{B_{ij}} F(x_i,y_j) + Err,$$

where $|Err| \leq M \cdot h^4/8 \cdot (2p)^2$. (The constant $M = \max \left\{ \left| \frac{\partial^4 F}{\partial u^4} \right|, \left| \frac{\partial^4 F}{\partial u^2 \cdot \partial v^2} \right|, \left| \frac{\partial^4 F}{\partial v^4} \right| \right\}$.)

Proof:

Except for the fact that a 2-dimensional version of Taylor's Theorem is necessary, the proof of this theorem is the same as the familiar Simpson's Rule.

Since the functions $F(u,v)$ to be integrated in this paper are $X(u,v)$ or $Y(u,v)$ convolved with Θ_p, $F(u,v) = 0$ whenever $u = \pm p$ or $v = \pm p$. Thus, for the purposes of this paper $\iint_{R_p} F(u,v)dudv$ $\tfrac{4}{3}h^2 \cdot \sum_{Aij} R(x_i,y_j)$. For the applications illustrated in this paper h was chosen to be $p/4$. This choice of h is equivalent to

dividing the square into 16 equal pieces. To approximate the integral of F when h = p/4 the function must be evaluated at 40 points. See Figure 5.

The following example has been worked out to illustrate how the theory from the provious section can be applied to a specific transformation. The equations given below approximate the projection of one half of the X-24C aircraft into the plane. The transformation to be smoothed is $T(u,v) = (X(u,v), Y(u,v))$ where $X(u,v)$ and $Y(u,v)$ are defined below.

If $u \le 1$, $X(u,v) = u$ and $Y(u,v) = 2v$.

If $1 \le u \le 2$, $X(u,v) = -13 + 14u + .8u - .8uv$ and

$Y(u,v) = -3.5 + 3.5u + 1.9v + (.1)uv$.

If $2 \le u \le 3$, $X(u,v) = 7 + 4u - 1.15v + .175uv$ and

$Y(u,v) = -.5 + 2u + 1.3v + .4uv$.

Let $F(u,v) = \sqrt{\sqrt{u^2 + v^2} + u}$.

Let $A = 22 - \sqrt{2}/4F(1,v)^3 + 3\sqrt{2}/4 \cdot v \cdot F(-1,v)$,

$B = 76 - 19u - 2.5v + .625uv$,

$C = 5.5 - \sqrt{2}/4F(-1,v)^3 + 3\sqrt{2}/4 \cdot v \cdot F(1,v)$, and

$D = 22 - 5.5u + 10v - 2.5uv$.

If $3 \le u \le 4$, $X(u,v) = (u-3)A + B$ and $Y(u,v) = (u-3)C + D$.

If $u \ge 4$, $X(u,v) = 22 - \sqrt{2}/4 \cdot F(5-u,v)^3 + 3\sqrt{2}/4 \cdot v \cdot F(u-5,v)$ and

$Y(u,v) = 5.5 - \sqrt{2}/4F(u-5,v)^3 + 3 \cdot v \cdot F(5-u,v)\sqrt{2}/4$.

Note that the transformation on the region $u \ge 4$ is nothing more than a translated and rotated version of the map $w = z^{3/2}$. For $3 \le u \le 4$ the transformation is an interpolation between a straight line and the $w = z^{3/2}$ map. The grid for this transformation is illustrated in Figure 4. Note the singularities of the first

derivative along the lines u=1, u=2, u=3, and u=4. A smoothed version of this grid is seen in Figure 5. This grid was generated by convolving T with the bump function $\theta_p(u,v)$ where p = 0.5. Note that the singularities have now disappeared.

IV. Concluding Remarks

The mathematics in this paper shows that it is possible to patch a grid together from local grids. Even if the "patched" grid is not smooth, it can be approximated by a smooth one. Desirable properties such as orthogonality and appropriate clustering of grid points will be almost retained. While this approximation technique will never produce grids as "perfect" as those generated by conformal or hyperbolic techniques, it should be useful in piecing together complicated configurations where one is more interested in obtaining a "reasonable" grid rather than a flawless one. Once the equations for the grid in each section have been obtained, the method is very fast. Also, since the convolutions are evaluated locally there is no accumulated error. (i.e. Errors incurred in calculating one grid point do not enter into the calculating of the next.) The examples illustrated were all run single precision. Obviously, if more accuracy is warrented, the computer programs could be run with double precision and with a larger selection of points when applying Simpon's Rule.

When applying the smoothing techniques indicated in this paper, care must be used when choosing the value of the parameter p. If p is too large the approximation will not be close enough. Thus, the Jacobian could become zero or the control on orthogonality could be lost. If p is small relative to the number of grid points, the grid will have "numerical discontinuities" in the derivatives.

One final remark should be made. The parameter p does not

have to be a constant. If very tight fit of grid lines is needed at some point, the parameter p can be allowed to approach zero. This new convolution will still be C^{∞} if p is constant near points of discontinuities of the partial derivatives of the transformation. If p varies arbitrarily the new transformation will only be C^{1}.

Acknowledgement

The author would like to acknowledge Will Hanky and Joe Shang of the Flight Dynamics Lab at Wright - Patterson AFB. Without their guidance and encouragement this research would not have been possible. Thanks also to Steve Scheer for his help with the graphics.

References

1. Smith, R.E., "Algebraic Grid Generation," Numerical Grid Generation, Proceedings of a symposium on the Numerical Generation of Curvilinear Coordinate Systems and their use in the Numerical Solution of Partial Differential Equations, Nashville, Tennessee, April 1982.

2. Hirsch, M.W., Differential Topology, Graduate Texts in Mathematics, Springer - Verlag, 1976.

3. Munkres, J.R., Elementary Differential Topology, Annals of Mathematics Studies Number 54, Princeton University Press, Princeton, New Jersey, 1966.

4. Rudin, W., Principles of Mathematical Analysis, 2nd Ed., McGraw - Hill, 1964.

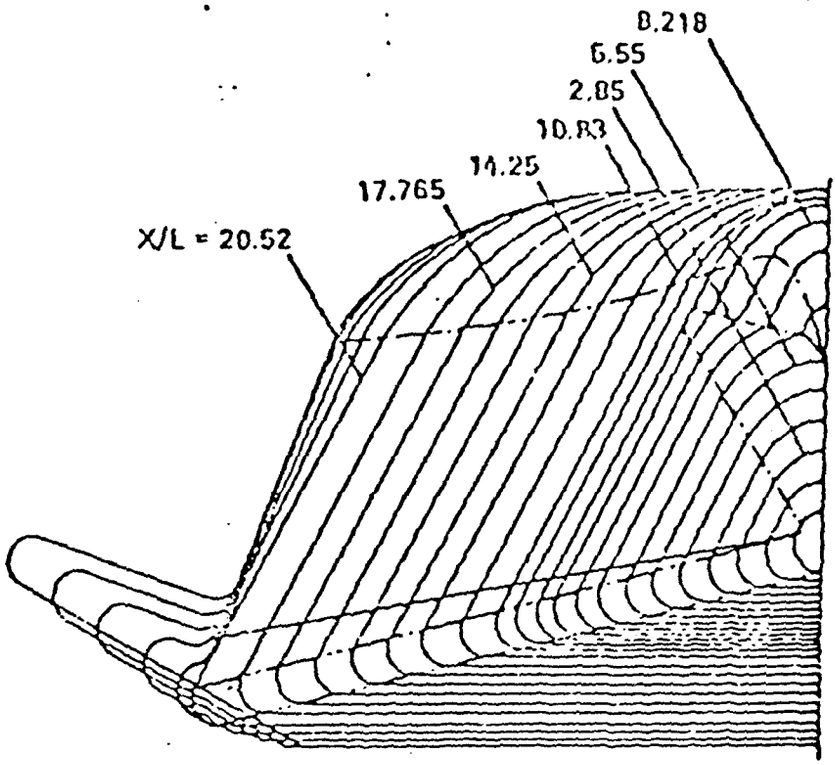

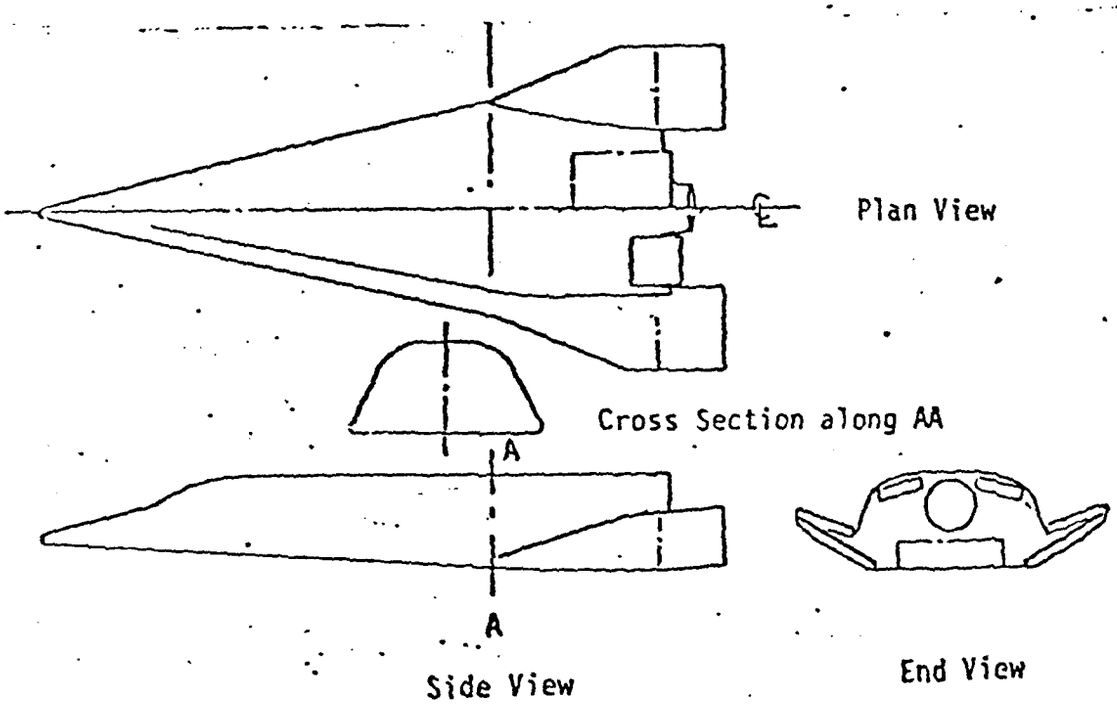

Three Views of X-24C Configuration.

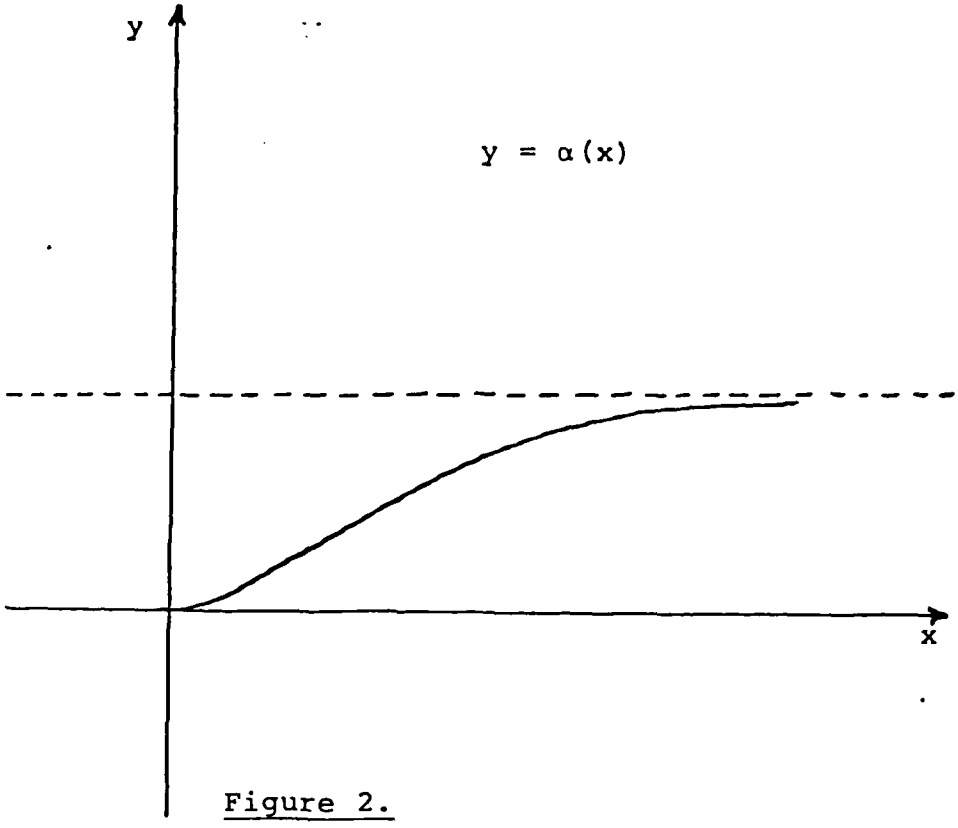

Figure 2.

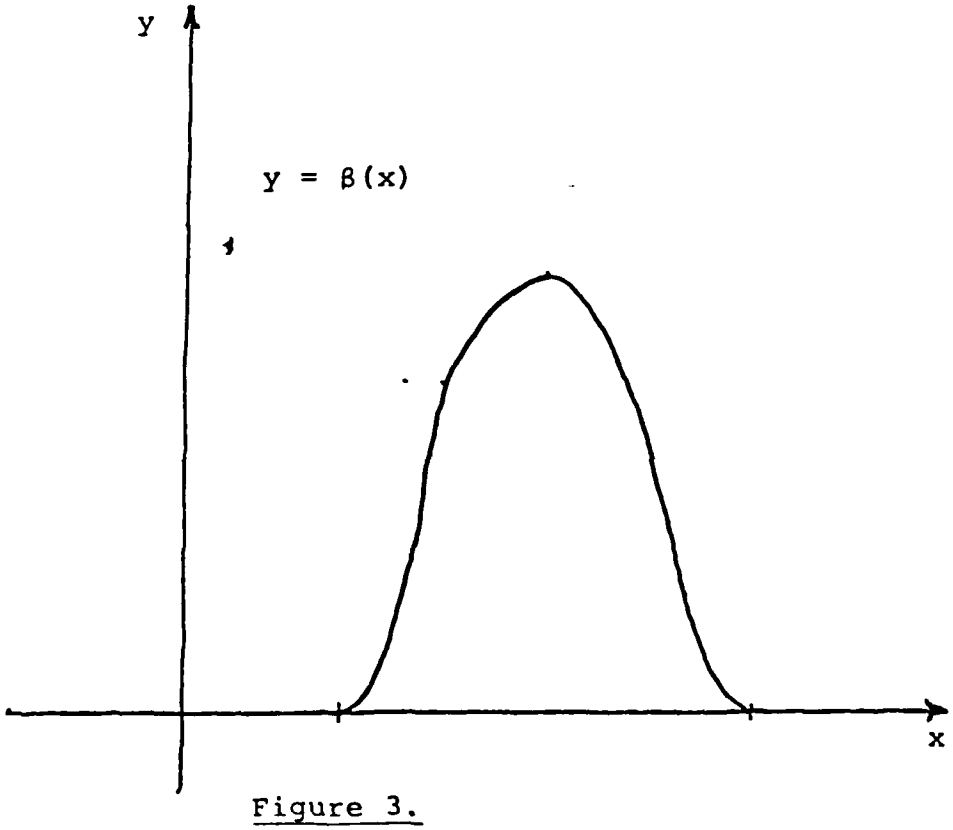

Figure 3.

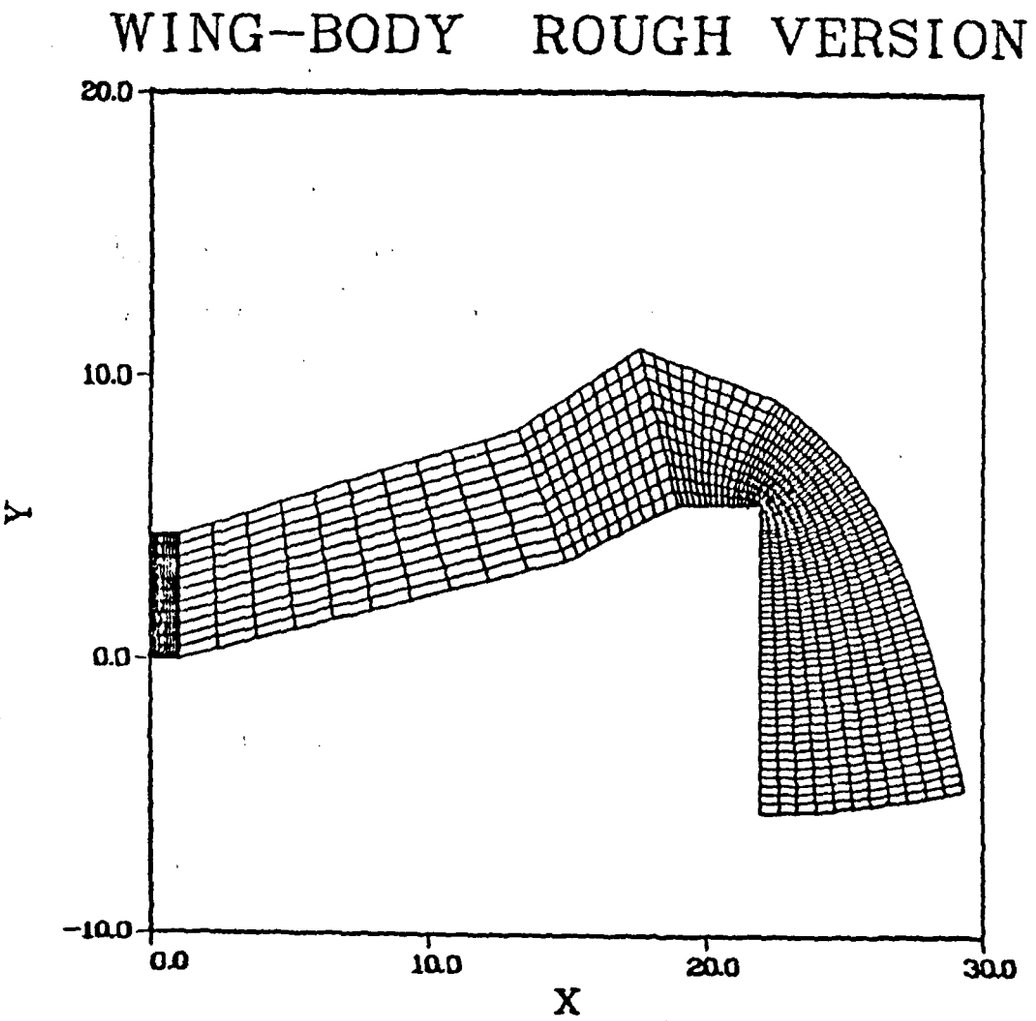

Figure 4.

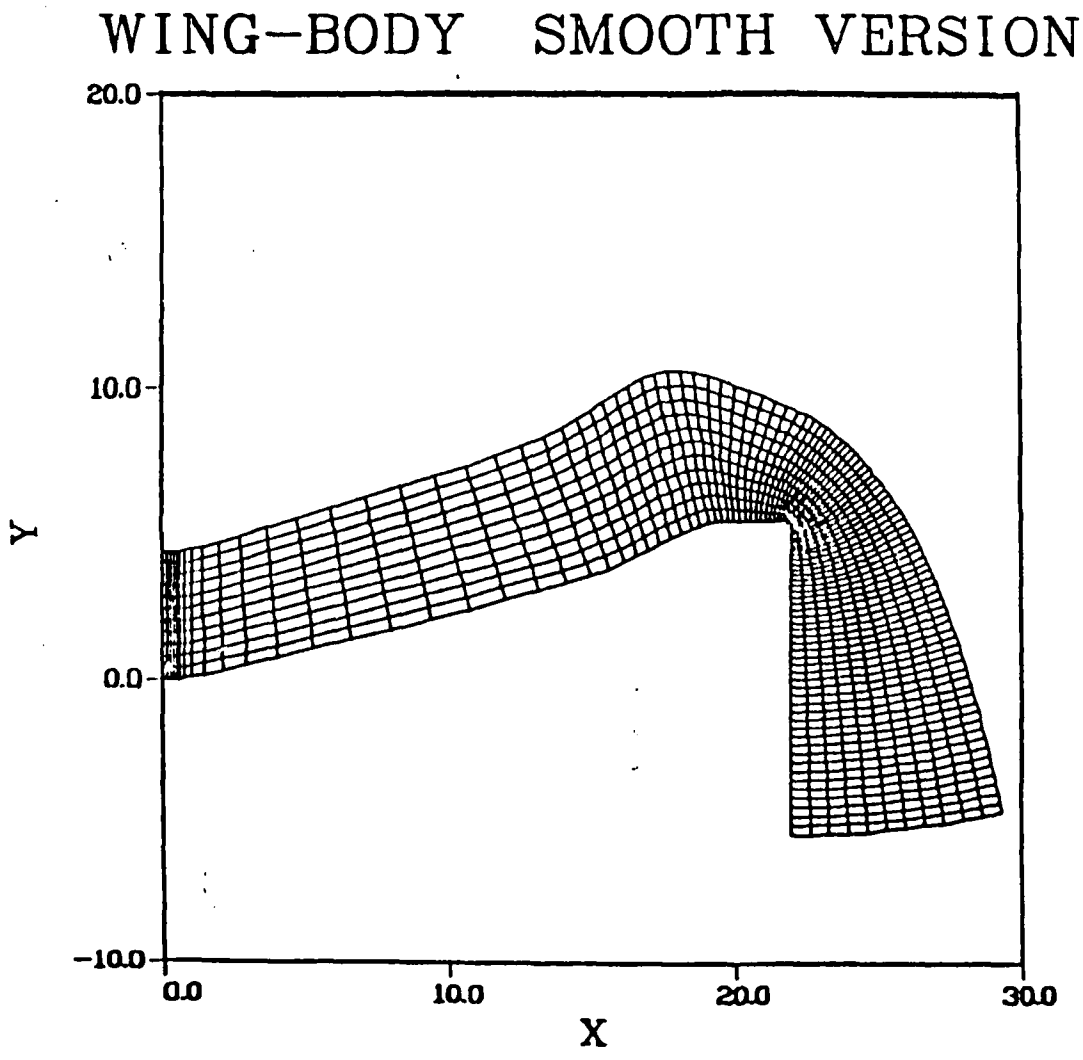

Figure 5.

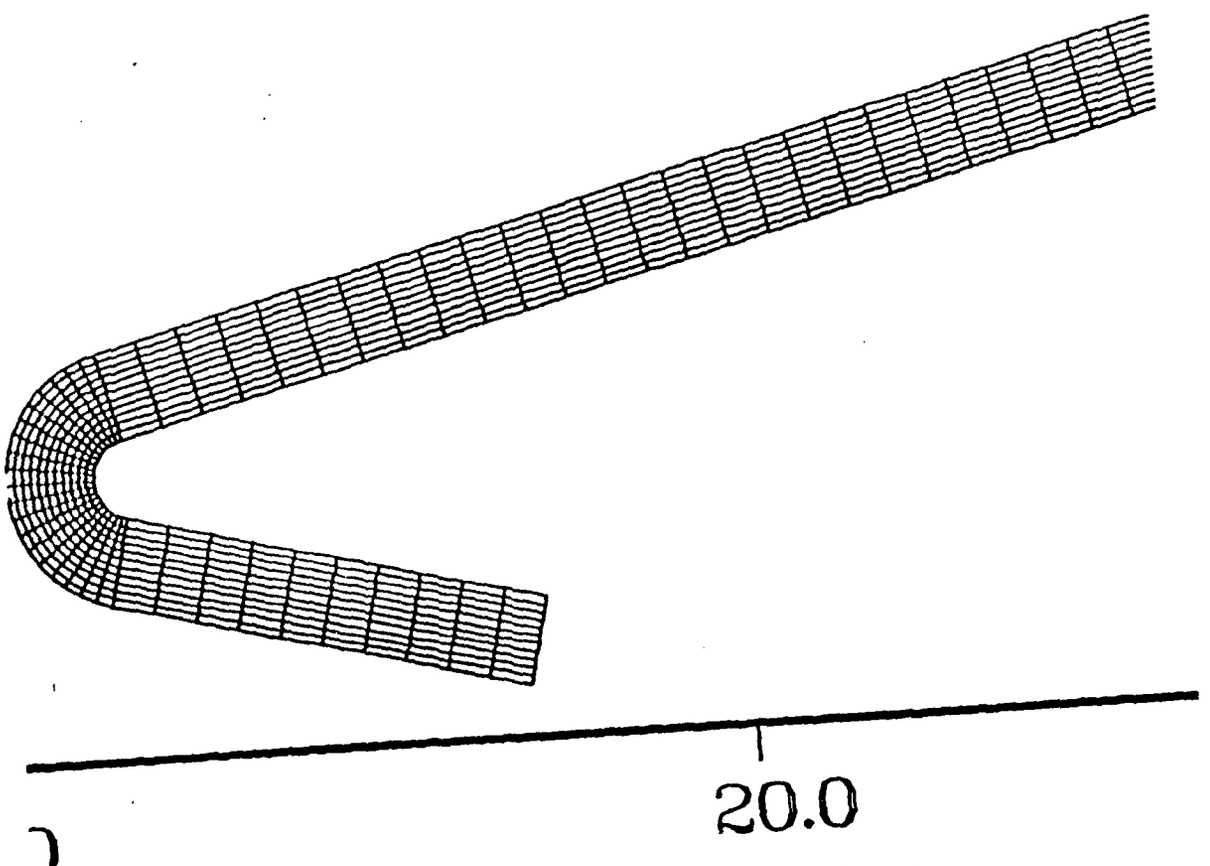

Figure 6.

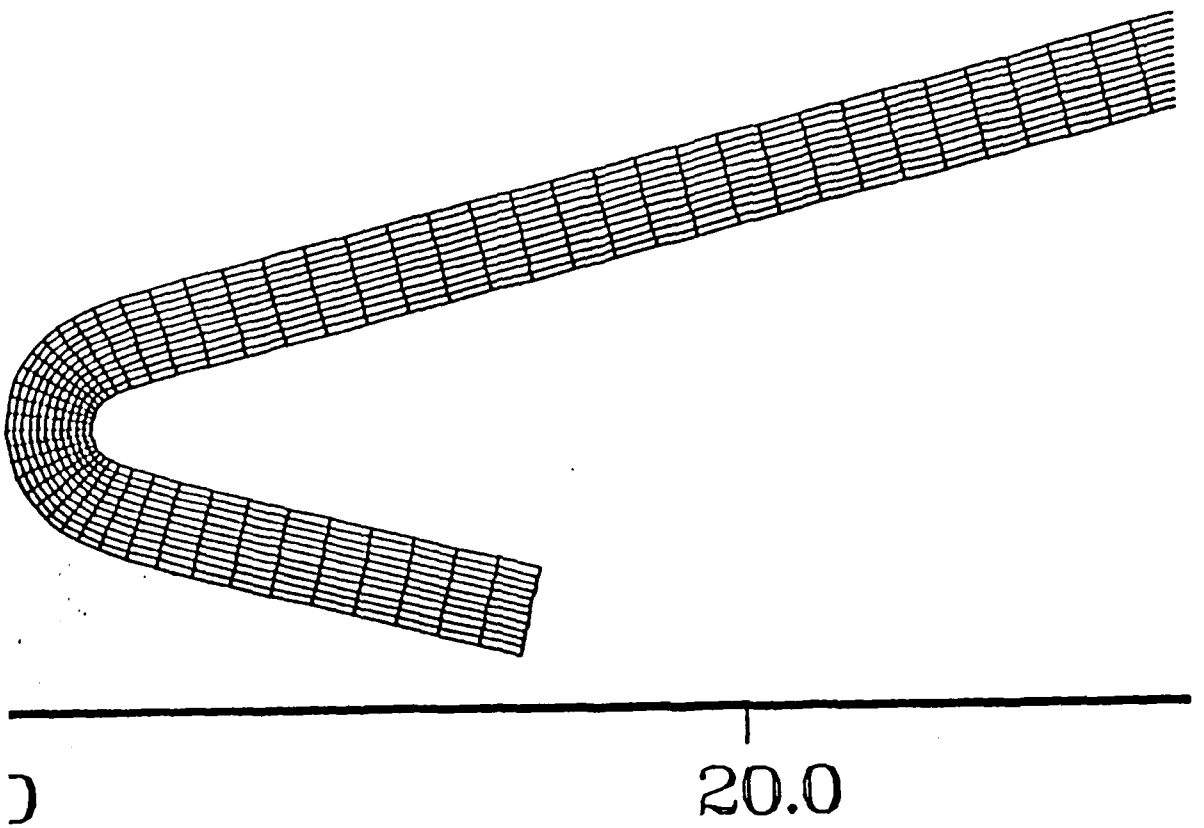

Figure 7.

REVISED 12/84

SMOOTHING PATCHED GRIDS

David C. Wilson
Mathematics Department
University of Florida, Gainesville, Florida 32611

Abstract

The purpose of this paper is to indicate how smoothing techniques can be utilized in the area of grid generation. The focus of the paper is to show how one global grid can be patched together from a number of smaller ones. The procedure usually takes place in two steps. First, one global grid is patched together from a number of smaller ones, allowing for the possibility that the derivatives along common boundaries may not be continuous. The second step is to then approximate this grid by a smooth one in such a way that the essential structure of each patch is preserved.

This research was supported in part by AFOSR Grant #83-0158. The paper was revised while the author was an ASEE Fellow at NASA Langley during the Summer of 1984.

I. Introduction

The author developed the ideas outlined in this paper while attempting to construct a grid for an aircraft. A plane can be divided in a natural way into components such as the forebody, the airfoil, the tail, etc. The regions surrounding these components can usually be subdivided in a natural way so that suitable local grids (or patches) can be found for each subregion. However, the frustration of trying to splice together these various pieces into one global grid drove the author to search for a technique which would blend one patch into the next while still preserving the essential structure of each local grid. The principal smoothing technique described here involves a convolution of the grid transformation with a "bump" function to obtain a new smoother grid which approximates the old one. Each new grid point can be thought of as a weighted average of nearby points.

In this paper no effort will be made to deal with patches that overlap as Steger, Dougherty, and Benek [1] have done. In fact the standing assumption will be that adjacent patches will have common boundary. Moreover, the grid points on a common boundary between two adjacent regions will be assumed to agree. In the terminology of M. M. Rai [2] the grid may have metric discontinuities but no discontinuities. Figure 1 indicates the difference. (The author would prefer to say the grid is continous but not smooth.)

Actually, the problem of smoothing grids has been encountered before. For example, the elliptic method [3] or [4] can be thought of as a smoothing technique. The reason for this is that before the iterative scheme is to begin, the user must provide an initial guess (smooth or not). With good forture this guess is then rapidly molded into a smooth grid. Even simpler is the Laplace operator

$$X_n(I,J) = [X_{n-1}(I, J - 1) + X_{n-1}(I, J + 1) + X_{n-1}(I - 1, J) + X_{n-1}(I + 1, J)]/4.$$

A few iterations with this operator and a grid can be smoothed significantly. However, too many iterations may lead to a grid which is not one-to-one. Examples illustrating this difficulty are discussed in Section III. Kowalski [5] has developed a variation of the Laplace operator to smooth an algebraic grid. He allowed his operator to sweep through the grid as many as 12 times.

II. The Smoothing Theory

In order to explain the examples presented in Section III it is first necessary to present the background to the smoothing theory. While grid generation is primarily concerned with a discrete set of lattice points, it will be convenient here to present the theory in terms of continuous functions, derivatives, and integrals. The transition from the continuous theory to the discrete theory will be explained in Section III.

To develop the smoothing theory it is first necessary to explain the term "bump" function. If R denotes the real numbers and $p > 0$, then a nonnegative function $\theta_p : R \to (0,\infty)$ is a bump function supported on the interval $[-p,p]$ if it is smooth, is identically zero outside $[-p,p]$, and has the property that

$$\int_{-p}^{p} \theta_p(x)\, dx = \int_{-\infty}^{\infty} \theta_p(x)\, dx = 1.$$

While there are innumerable choices for a bump function, the one indicated below is convenient to explain and use.

First define the function $\alpha:R \to [0,\infty)$ by the rule

$$\alpha(x) = \begin{cases} 0 & \text{if } x \leq 0 \\ e^{-1/x} & \text{if } x > 0 \end{cases}.$$

Note that α is C^∞ and identically zero on $(-\infty,0]$. The graph of α is indicated in Figure 2. If $\beta_p(x) = \alpha(x - p) \cdot \alpha(p - x)$, then β_p is nonnegative, is identically zero off the interval $[-p,p]$, and is C^∞. The graph of β_p is indicated in Figure 3. If $A_p = \int_{-p}^{p} \beta(x)\, dx$ and $\theta_p(x) = \beta_p(x)/A_p$, then $\theta_p(x)$ is a bump function supported on $[-p,p]$.

Since grid generation is primarily concerned with arrays in 2 and 3 dimensions, the notion of bump function must be extended to the square $R_p = [-p,p] \times [-p,p]$. Note that $\theta_p(x,y) = \theta_p(x) \cdot \theta_p(y)$ is nonnegative, is identically zero off R_p, and is C^∞. Note also that $\iint_{R_p} \theta_p(x,y)\, dx\, dy = 1$.

Definition: If $F(\xi,\eta)$ is a piecewise continuous function from $R^2 \to R$, then the convolution of F by θ_p is defined by the equation

$$\theta_p * F(\xi,\eta) = \iint_{R_p} F(\xi - u,\ \eta - v) \cdot \theta_p(u,v)\, du\, dv\ .$$

Intuitively, the convolution can be thought of as an average of the values of F over the square $[\xi - p,\ \xi + p] \times [\eta - p,\ \eta + p]$ relative to the weight function $\theta_p(u,v)$. In particular, if $F(x,y) = 1$ for all $(x,y) \in R^2$, then $\theta_p * F(\xi,\eta) = 1$ for all ξ,η. Thus, it becomes clear that if F is nearly constant near (ξ,η), then $\theta_p * F(\xi,\eta)$ is "close" to $F(\xi,\eta)$. Theorem 2.1 gives a precise statement of this observation. In fact Theorems 2.1-2.9 give precise formulations of the following statements.

1. If p is "small", then $\theta_p * F$ is "close" to F.
2. For any p, the convolution $\theta_p * F$ is a C^∞ function.
3. If $F(\xi,\eta)$ is differentiable at (ξ,η) and p is small, then all the derivatives of $\theta_p * F(\xi,\eta)$ will be close to the derivatives of $F(\xi,\eta)$.
4. If $T(\xi,\eta) = (X(\xi,\eta), Y(\xi,\eta))$, the Jacobian J of T is not zero, and p is small, then the Jacobian J_p of $\theta_p * T$ is not zero.
5. If T is orthogonal and p is small, then $\theta_p * T$ is "nearly" orthogonal.
6. The convolution operator is linear.

7. The convolution operator is invariant when applied to functions of the form $F(x,y) = A + Bx + Cy + Dxy$.

At this point the reader who is not interested in the theory can skip ahead to the examples in Section III. An excellent reference for the Advanced Calculus needed in the proofs of the following theorems is Rudin [6]. Theorems 2.1-2.3 are lifted directly from the Differential Topology books by Hirsch [7] and Munkres [8].

Theorem 2.1 If F is continuous, $\varepsilon > 0$, and $|F(\xi - u, \eta - v) - F(\xi,\eta)] < \varepsilon$ for all $(u,v) \in R_p$, then $|\theta_p * F(\xi,\eta) - F(\xi,\eta)| < \varepsilon$.

Proof

The result follows from the following sequence of equalities and inequalities.

$$|\theta_p * F(\xi,\eta) - F(\xi,\eta)|$$

$$= \left|\iint_{R_p} F(\xi - u, \eta - v)\ \theta_p(u,v)\ dudv - F(\xi,\eta)\right|$$

$$< \iint_{R_p} \theta_p(u,v) \cdot |F(\xi - u, \eta - v) - F(\xi,\eta)|\ dudv$$

$$< \varepsilon \iint_{R_p} \theta_p(u,v)\ dudv = \varepsilon.$$

Theorem 2.2 If $F(\xi,\eta)$ is piecewise continuous, then $\theta_p * F(\xi,\eta)$ is C^∞.

Proof

By change of variables we have

$$\frac{\partial \theta_p * F(\xi,\eta)}{\partial \xi} = \frac{\partial}{\partial \xi} \iint_{R_p} \theta_p(u,v) \cdot F(\xi - u,\ \eta - v)\ dudv$$

$$= \frac{\partial}{\partial \xi} \int_{\eta-p}^{\eta+p} \int_{\xi-p}^{\xi+p} \theta_p(\xi + u,\ \eta + v)\ F(u,v)\ dudv$$

$$= \int_{\eta-p}^{\eta+p} \int_{\xi-p}^{\xi+p} \frac{\partial \theta_p(\xi + u,\ \eta + v)}{\partial \xi} \cdot F(u,v)\ dudv.$$

Since θ_p is C^∞, $\theta_p * F$ is C^∞.

Theorem 2.3 shows that if p is "small" and $\frac{\partial F(\xi,\eta)}{\partial \xi}$ is continuous at (ξ,η), then $\frac{\partial \theta_p * F(\xi,\eta)}{\partial \xi}$ is "close" to $\frac{\partial F(\xi,\eta)}{\partial \xi}$. Note that Theorem 2.3 can be easily generalized to higher derivatives.

Theorem 2.3 If $F(\xi,\eta)$ is C^1, then $\frac{\partial \theta_p * F(\xi,\eta)}{\partial \xi} = \theta_p * \frac{\partial F(\xi,\eta)}{\partial \xi}$. Moreover, if $\varepsilon > 0$ and $\left|\frac{\partial F(\xi - u,\ \eta - v)}{\partial \xi} - \frac{\partial F(\xi,\eta)}{\partial \xi}\right| < \varepsilon$ for $(u,v) \in R_p$, then $\left|\frac{\partial \theta_p * F(\xi,\eta)}{\partial \xi} - \frac{\partial F(\xi,\eta)}{\partial \xi}\right| < \varepsilon$.

Proof

Since $\frac{\partial}{\partial \xi} \iint_{R_p} \theta_p(u,v) \cdot F(\xi - u,\ \eta - v)dudv = \iint_{R_p} \theta_p(u,v) \cdot \frac{\partial F(\xi - u,\ \eta - v)}{\partial \xi}\ dudv$, $\frac{\partial \theta_p * F(\xi,\eta)}{\partial \xi} = \theta_p * \frac{\partial F(\xi,\eta)}{\partial \xi}$. The second half of the theorem follows from the proof of Theorem 2.1.

Remark

Theorem 2.3 could have been phrased as follows: If $\frac{\partial F}{\partial \xi}$ is piecewise continuous and $m < \frac{\partial F}{\partial \xi} < M$, then $m < \theta_p * \frac{\partial F}{\partial \xi} < M$. Thus, at points where

$\frac{\partial F}{\partial \xi}$ is not continuous, the convolution of F by θ_p "blends" the first partials of the grid in one section into those of the next. This blending also occurs for all higher derivatives. Theorem 2.4 ensures that if T is one-to-one and p is "small", then $\theta_p * T$ is one-to-one.

Theorem 2.4 If $T(\xi,\eta) = (X(\xi,\eta), Y(\xi,\eta))$ where $X(\xi,\eta)$ and $Y(\xi,\eta)$ are C^1, then if the Jacobian J of T is not zero there is a $p > 0$ such that the Jacobian J_p of $\theta_p * T(\xi,\eta) = (\theta_p * X(\xi,\eta), \theta_p * Y(\xi,\eta))$ is not zero.

Proof

The Jacobian $J_p = \left(\theta_p * \frac{\partial X}{\partial \xi}\right) \cdot \left(\theta_p * \frac{\partial Y}{\partial \eta}\right) - \left(\theta_p * \frac{\partial X}{\partial \eta}\right) \cdot \left(\theta_p * \frac{\partial Y}{\partial \xi}\right)$.

By Theorem 2.3. $\lim_{p \to 0} J_p = J$.

Theorem 2.5 Let $T(\xi,\eta) = (X(\xi,\eta), Y(\xi,\eta))$ be a C^1 transformation and let Ψ be the angle between $u = \left(\frac{\partial X}{\partial \xi}, \frac{\partial Y}{\partial \xi}\right)$, and $v = \left(\frac{\partial X}{\partial \eta}, \frac{\partial Y}{\partial \eta}\right)$. If Ψ_p denotes the angle between $u_p = \left(\theta_p * \frac{\partial X}{\partial \xi}, \theta_p * \frac{\partial Y}{\partial \xi}\right)$ and $v_p = \left(\theta_p * \frac{\partial X}{\partial \eta}, \theta_p * \frac{\partial Y}{\partial \eta}\right)$, then $\lim_{p \to 0} \Psi_p = \Psi$.

Proof

By Theorem 2.3 $\lim_{p \to 0} u_p = u$ and $\lim_{p \to 0} v_p = v$. Since $\cos \Psi_p = \frac{u_p \cdot v_p}{|u_p| \cdot |v_p|}$ and $\cos \Psi = \frac{(u \cdot v)}{|u| \cdot |v|}$, $\lim_{p \to 0} \Psi_p = \Psi$.

Theorem 2.6. If $F(\xi,\eta) = F_1(\xi,\eta) + F_2(\xi,\eta)$, where F_1 and F_2 are piecewise continuous, then $\theta_p * F(\xi,\eta) = \theta_p * F_1(\xi,\eta) + \theta_p * F_2(\xi,\eta)$.

Proof

The additivity of the integral is all that is needed to prove this theorem.

Theorem 2.7 If $F(\xi,\eta) = f(\xi) \cdot g(\eta)$, where f and g are piecewise continuous, then $\theta_p * F(\xi,\eta) = [\theta_p * f(\xi)] \cdot [\theta_p * g(\eta)]$.

Proof

This result is an immediate consequence of Fubini's Theorem.

Theorem 2.8 If $F(\xi,\eta) = A + B\xi + C\eta + D\xi\eta$, then $\theta_p * F(\xi,\eta) = F(\xi,\eta)$.

Proof

It is a routine check to show that if $G(\xi,\eta) = \xi$, then $\theta_p * G(\xi,\eta) = G(\xi,\eta)$. The theorem is now an immediate consequence of Theorems 2.6 and 2.7.

Theorem 2.8 shows that if a portion of the grid of the aircraft can be defined by equations of the form $F(\xi,\eta) = A + B\xi + C\eta + D\xi\eta$, then the convolution step can be bypassed. Thus, the grid can be generated much more rapidly in that region.

The next theorem is of interest because it gives sufficient conditions which ensure that the Jacobian will be nonzero at (ξ,η) even in the case that the partial derivatives of $T(\xi,\eta)$ are not defined at (ξ,η). In most applications these hypotheses will be satisfied.

Theorem 2.9 If $T(\xi,\eta) = (X(\xi,\eta), Y(\xi,\eta))$ has piecewise continuous partials and $ad - bc > 0$, where $a < \frac{\partial X}{\partial \xi}$, $\frac{\partial X}{\partial \eta} < b$, $\frac{\partial Y}{\partial \xi} < c$, and $d < \frac{\partial Y}{\partial \eta}$ for all points in $(u - p, u + p) \times (v - p, v + p)$, then the Jacobian J_p of $\theta_p * T$ is nonzero.

Proof

By the remark after Theorem 2.3 $a < \theta_p * \frac{\partial X}{\partial \xi}$, $\theta_p * \frac{\partial X}{\partial \eta} < b$, $\theta_p * \frac{\partial Y}{\partial \xi} < c$, and $d < \theta_p * \frac{\partial Y}{\partial \eta}$ so that

$$J_p = \left(\theta_p * \frac{\partial X}{\partial \xi}\right) \cdot \left(\theta_p * \frac{\partial Y}{\partial \eta}\right) - \left(\theta_p * \frac{\partial X}{\partial \eta}\right) \cdot \left(\theta_p * \frac{\partial Y}{\partial \xi}\right) > ad - bc > 0.$$

One final remark should be made at this point. While all the theorems in this section have been stated in a two-dimensional setting, each one generalizes to three dimensions.

III. The Examples

The purpose of this section is to indicate how the theory from Section II can be applied to smooth a patched grid. Immediately, we are confronted with four problems.

1. The size of the parameter p must be fixed.
2. The bump function must be selected.
3. A numerical integration technique must be chosen.
4. A method must be found to fix the points on the boundary, while retaining the overall smoothness of the rest of the grid.

In the discrete setting the point (ξ,η) must be replaced by the lattice point (I,J), where I and J are integers. Since the choice of the parameter p determines the size of the square R_p, the selection of p now becomes a decision concerning the number of neighbors of (I,J) to be used when convolving with the bump function. If the point (I,J) is to be in the center of the square, the reasonable choices seem to be 9,25,49, etc. In the discrete situation the larger the number of points, the smoother the new grid will be. However, the increased number of computations could easily become prohibitive. For the purposes of the examples presented here the author chose 49 neighbors for each point (I,J). These 49 will be of the form $(I + K, J + K')$, where $|K| \leq 3$ and $|K'| \leq 3$.

While the choice of bump function is important, it does not seem to be as critical as some of the other problems. However, if one is careless and chooses a bump function which is very near zero except at the point (I,J), then very little or no smoothing will take place. Since the bump function is identically zero on the boundary of the square R_p, the integration is now to be performed over the square $(I + K, J + K')$, where $|K| \leq 2$ and $|K'| \leq 2$.

The method of integration chosen is the two-dimensional version of the Newton-Cotes formula indicated in Proposition 3.1. This two-dimensional integrator was obtained by discarding the remainder term and taking the tensor product with itself.

Proposition 3.1 (See page 93 of Hildebrand [9].) If $x_o < x_1 < \ldots < x_6$, $h = x_{i+1} - x_i$, and $f_i = f(x_i)$, then

$$\int_{x_o}^{x_6} f(x)\,dx = \frac{h}{140}(41f_o + 216f_1 + 27f_2 + 272f_3 + 27f_4 + 216f_5 + 41f_6) - \frac{9h^9}{1400} f^{(8)}(z).$$

In the theory outlined in Section II there is no mention of boundary points. If the problem is ignored, the surface of the aircraft will be smoothed along with the grid. Sharp corners will become rounded. (Compare Figs. 4 and 5.) While there are a variety of ways to deal with this problem, the author chose to reduce the amount of smoothing for grid points near the boundary by linear blending. In particular, if $T(I,J)$ denotes the original grid point and d is the distance from $T(I,J)$ to the boundary, then the new grid point will be $T_n(I,J) = dT_s(I,J) + (1 - d)\,T(I,J)$, where $T_s(I,J)$ denotes the corresponding point of the smoothed grid. Figures 6-10 indicate the rough and smooth versions of various shapes. Since the value of d was never quite equal to 1 in these examples, small discontinuities in the derivatives were propagated into the interior of the regions. Despite this problem the grids were still smoothed fairly well. In the future the author plans to develop a distance function which is exactly equal to 1 throughout most of the interior of the region so that the grid will be smooth away from the boundary.

Figures 11 and 12 have been included to compare the Laplace operator and the simple average of the nine immediate neighbors. While these two methods are both much faster than the convolution, they usually need to be iterated to be effective. When iterated without boundary control, the grid points may drift outside the region in question. This phenomenon is demonstrated by Figure 13. This same Figure also shows that a transformation which is a solution of Laplace's equation may fail to be one-to-one even if it is one-to-one on the boundary. If boundary control is forced on the Laplace operator, then the grid points will stay in the region. However, discontinuities in the derivatives may appear near the boundary as indicated in Figure 14. Figure 15 illustrates the result when the convolution operator is iterated twice. Obviously, any further iterations and the grid will become overlapping.

IV. Concluding Remarks

The mathematics in this paper shows that it is possible to patch a grid together from local grids. Even if the patched grid is not smooth, it can be approximated by a smooth one. Desirable properties such as orthogonality and clustering of grid points will be almost retained. These techniques can be thought of as postprocessors to remove discontinuities in the grid derivatives along the boundaries of adjacent patches. A future application could be the smoothing of grids created from patches, where one patch is generated by a hyperbolic method, a second by an elliptic method, a third by an algebraic method (see Ref. [10] or [11]), etc. The final grid would then be a smoothed version of the union of the patches.

One further remark seems to be in order. When the author began this research, he only considered the convolution operator. At the suggestion of P. Eiseman the Laplace operator was also considered. While both worked well, the Laplace operator is easier to program, faster in terms of CPU time, and seemed to generate somewhat smoother grids. A reason for using the convolution operator is that it seems to be better at preventing overlapping near the boundary. The Laplace operator can frequently be iterated successfully 5-10 times. The convolution works best when applied 1-2 times.

Acknowledgement

The author would like to acknowledge Will Hankey and Joe Shang of the Flight Dynamics Laboratory at Wright-Patterson AFB. Without their guidance and encouragement this research would not have been possible. I would also like to thank Bob Smith and Peter Eiseman for their helpful comments and suggestions.

References

1. Steger, J. L., Dougherty, F. C., Benek, J. A., "A Chimera Grid Scheme," Mini-Symposium on Advances in Grid Generation, ASME Applied, Bioengineering and Fluids Engineering Conf., Houston, Texas, June 20-22, 1983.

2. Rai, M. M., "A Conservative Treatment of Zonal Boundaries for Euler Equation Calculations," AIAA 22nd Aerospace Sciences Meeting, Reno, Nevada, 1984.

3. Thompson, J. F., Thames, F. C. , and Mastin, C. M., "Automatic Numerical Generation of Body-Fitted Curvilinear Coordinate System for Field Containing Any Number of Arbitrary Two-Dimensional Bodies," Journal of Computational Phys. 14 (1974), 299-319.

4. Thames, F. C., Thompson, J. F., Mastin, C. W., and Walker, R. L., "Numerical Solutions for Viscous and Potential Flow about Arbitrary Two-Dimensional Bodies Using Body-Fitted Coordinate Systems," Journal of Computational Phys. 24 (1977), 245-273.

5. Kowalski, E. J., "Boundary-Fitted Coordinate Systems for Arbitrary Computational Regions," NASA Conference Publication 2166, NASA Langley Research Center, 1980, 331-353.

6. Rudin, W., Principles of Mathematical Analysis, 2nd Ed., McGraw-Hill, 1964.

7. Hirsch, M. W., Differential Topology, Graduate Texts in Mathematics, Springer-Verlag, 1976.

8. Munkres, J. R., Elementary Differential Topology, Annals of Mathematics Studies Number 54, Princeton University Press, Princeton, New Jersey, 1966.

9. Hildebrand, F. B., Introduction to Numerical Analysis, 2nd Ed., McGraw-Hill, 1974.

10. Eiseman, P. R., "A Multi-Surface Method of Coordinate Generation," Journal of Computational Phys. 33 (1979), 118-150.

11. Smith, R. E., "Algebraic Grid Generation," Numerical Grid Generation, Proceedings of a Symposium on the Numerical Generation of Curvilinear Coordinate Systems and Their Use in the Numerical Solution of Partial Differential Equations, Nashville, Tennessee, April 1982.

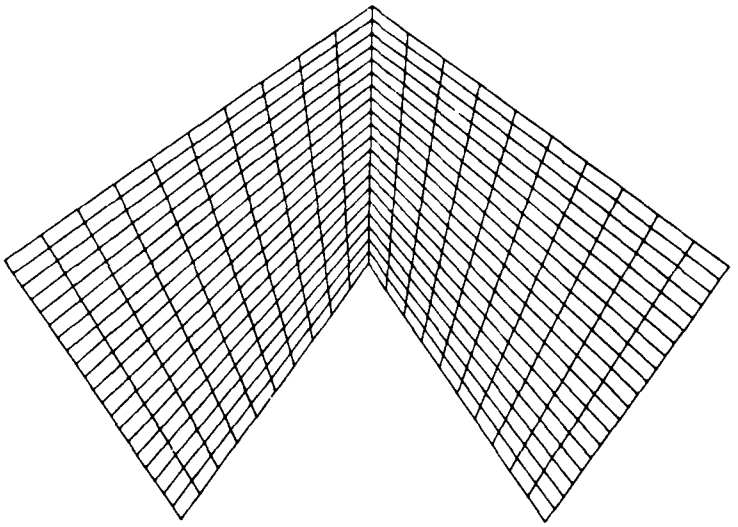

Figure 1a. Metric Discontinuity.

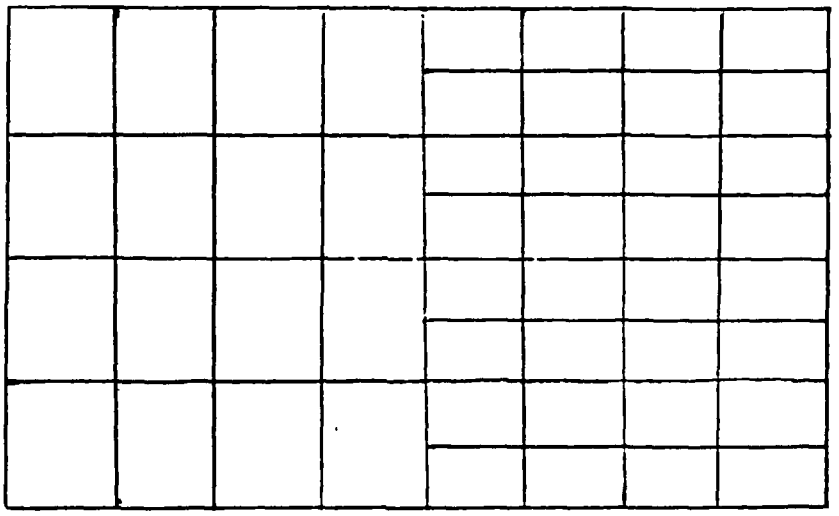

Figure 1b. Discontinuity

Figure 2. The Graph of the Function $\alpha(x)$.

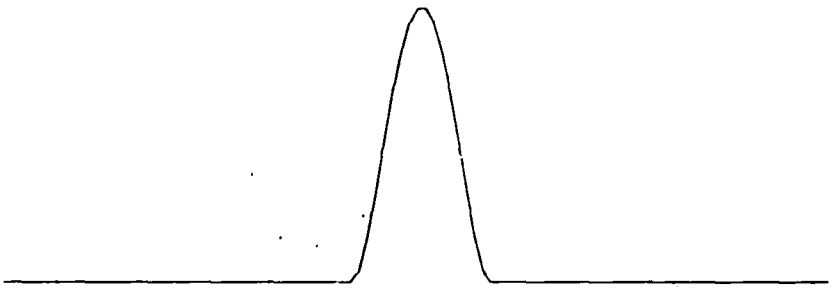

Figure 3. The Graph of the Function $\beta(x)$.

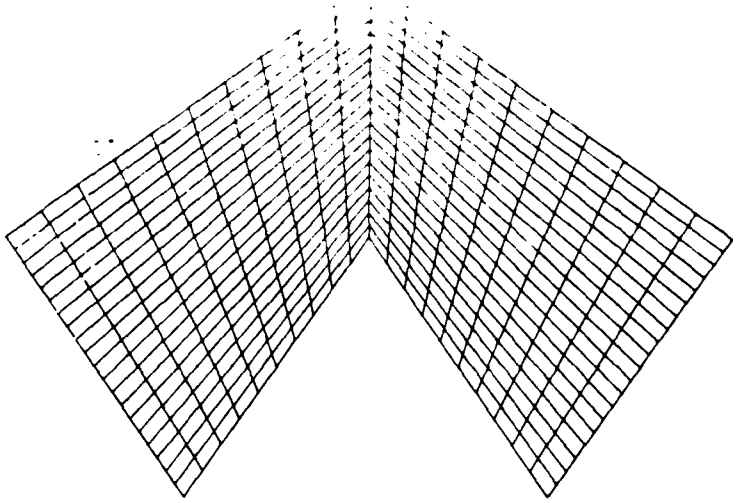

Figure 4. Corner-Before Smoothing.

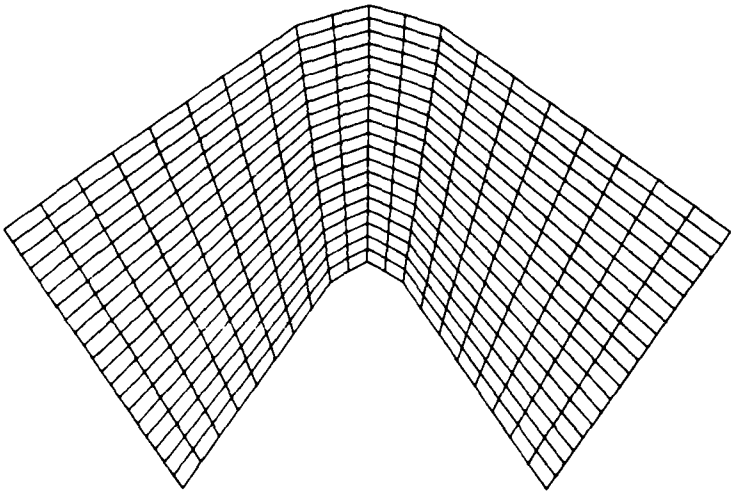

Figure 5. Corner-After Smoothing
(but without Boundary Control).

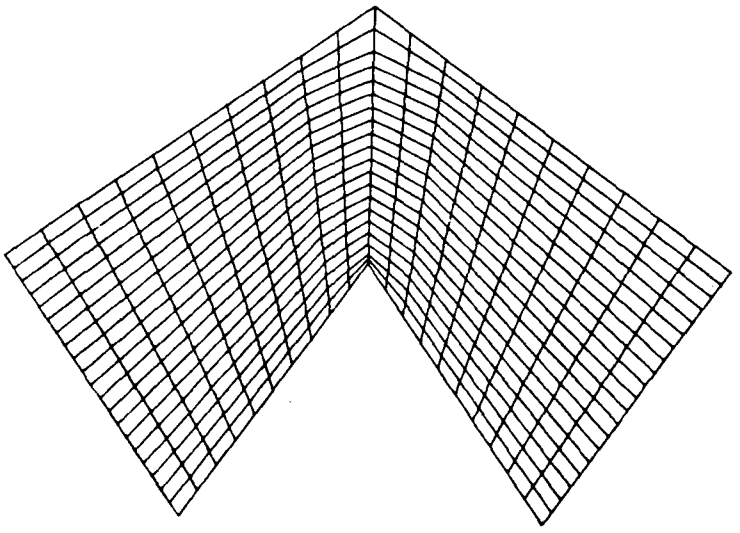

Figure 6. Corner-Smoothed with Boundary Control.

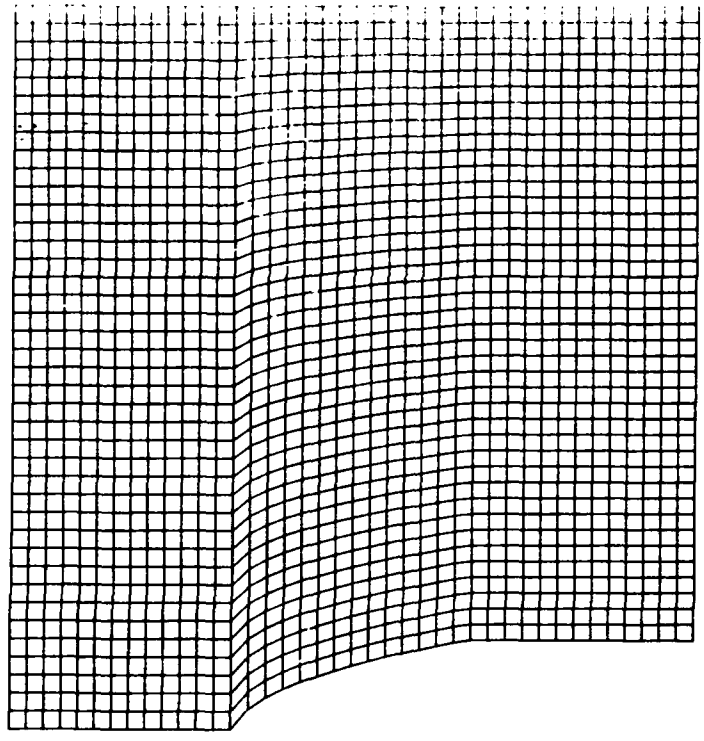

Figure 7. Foward Facing Ramp-Before Smoothing.

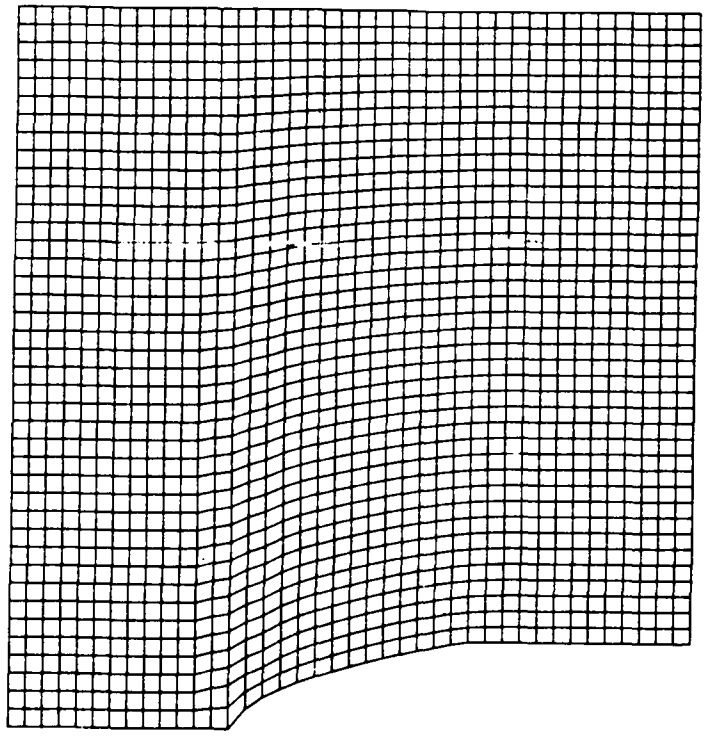

Figure 8. Forward Facing Ramp-After Smoothing.

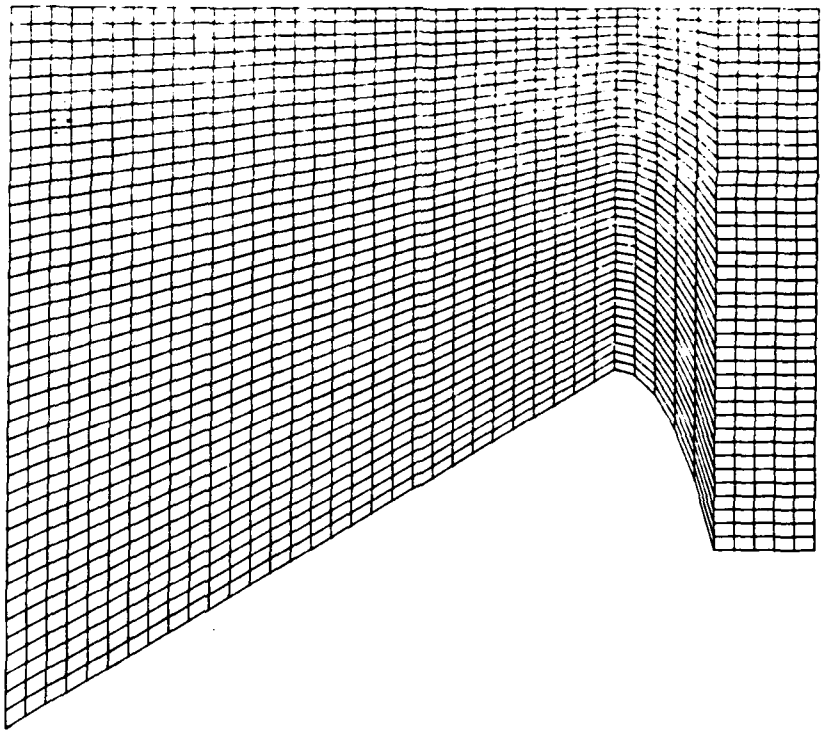

Figure 9. Bump-Before Smoothing.

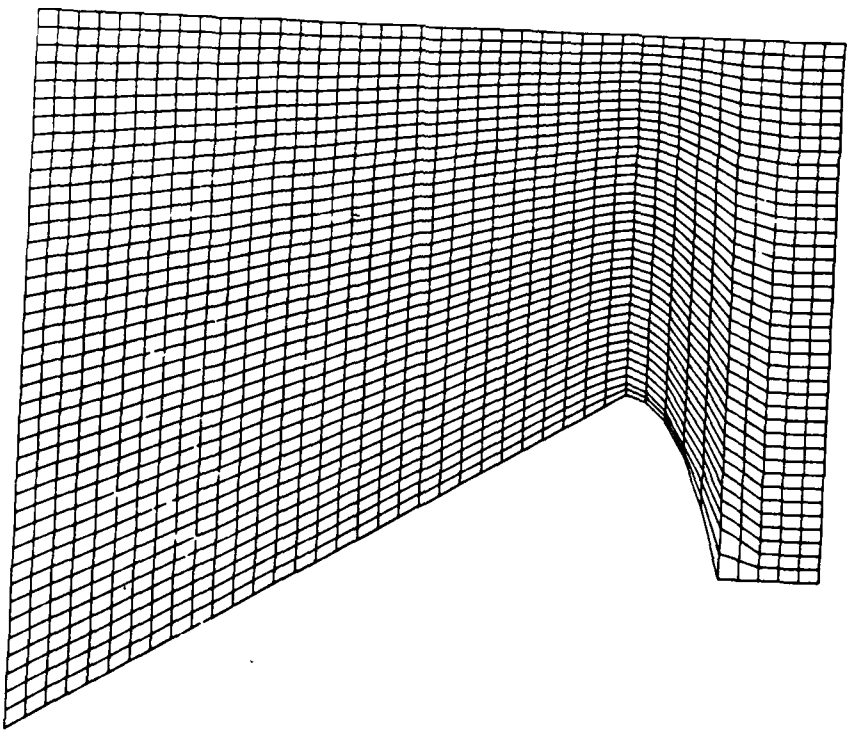

Figure 10. Bump-After Smoothing.

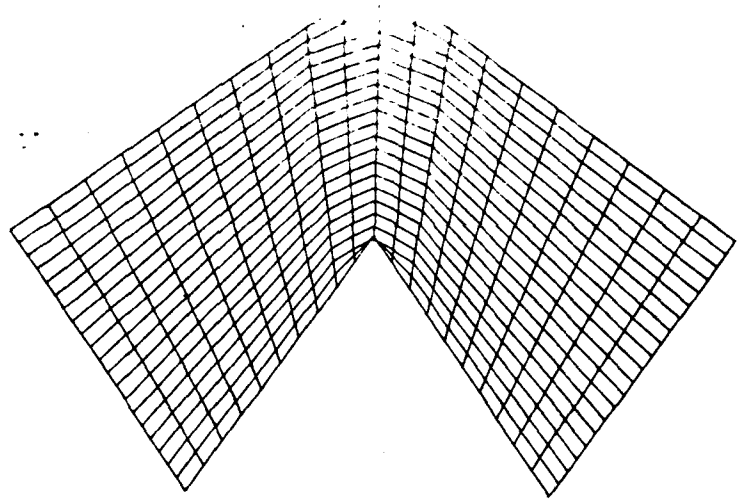

Figure 11. Corner-Smoothed by Laplace (with Boundary Control and 3 Iterations)

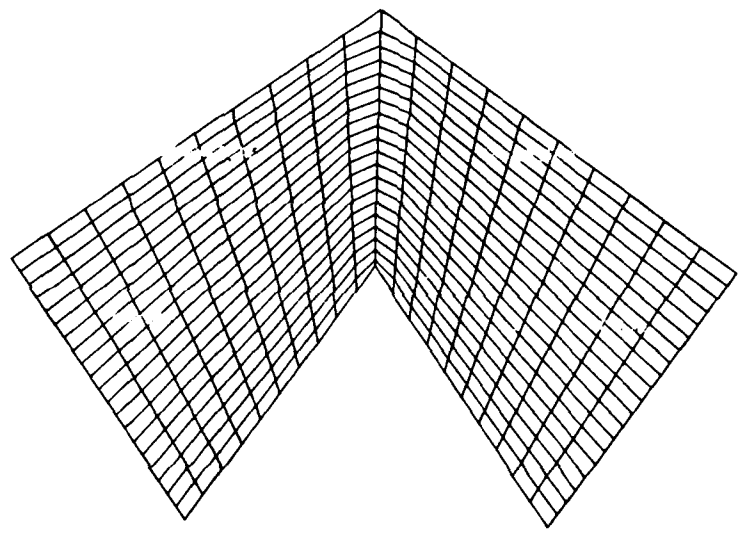

Figure 12. Corner-Smoothed by Nine Point Average.

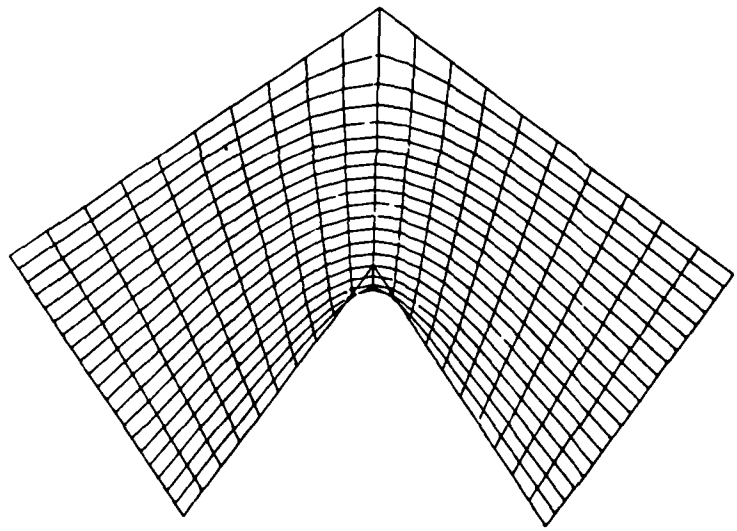

Figure 13. Corner-Smoothed by Laplace Operator (20 Iterations)

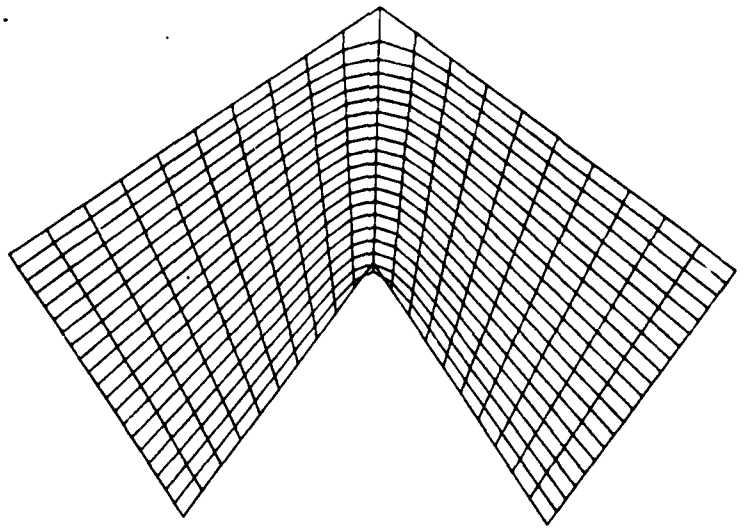

Figure 14. Corner-Smoothed by Laplace Operator (3 Iterations).

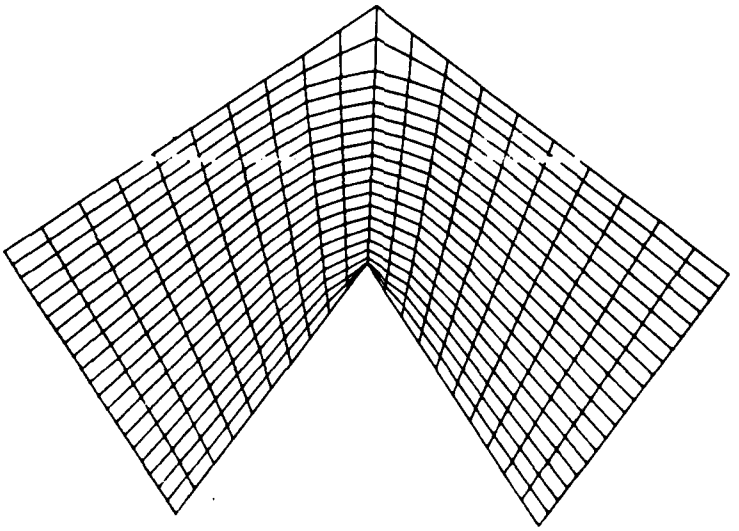

Figure 15. Corner-Smoothed with Boundary Control (2 Iterations).

END

FILMED

2-86

DTIC